DEVELOPMENT OF MOLTEN SALT REACTOR MODELING AND SIMULATION CAPABILITIES IN VERA

Aaron Graham[1*], Benjamin Collins[1], Robert Salko[1], Zack Taylor[2], Cole Gentry[1]

[1]*Oak Ridge National Laboratory*
1 Bethel Valley Road, Oak Ridge, TN 37830, USA

[2]*University of Tennessee*
Circle Park Drive, Knoxville, TN 37996, USA

[*]*grahamam@ornl.gov*, *collinsbs@ornl.gov*, *salkork@ornl.gov*, *mrtaylo45@vols.utk.edu*, *gentryca@ornl.gov*

In recent years, the nuclear community has seen a resurgence of interest in molten salt reactors (MSRs). Because of their molten, flowing fuel, MSRs present several new challenges not present in many other reactors, necessitating tightly coupled multiphysics modeling and simulation for accurate analysis. The Virtual Environment for Reactor Applications (VERA) has been developed to provide a high-fidelity multiphysics framework for reactor analysis. Though it was originally developed for light water reactor applications, VERA's multiphysics capabilities make for a natural extension to MSR analysis. Recent efforts have focused on capturing the effects of moving fuel. A lumped depletion capability has been added that accounts for the moving and mixing of the fuel, as well as time spent outside the active core. A general multi-phase species transport module has also been added to track the movement and evolution of salt constituents as the salt flows through the core and around the primary loop. This paper presents a discussion of the new MSR capabilities in VERA, along with results for the lumped depletion and species transport capabilities for the Molten Salt Reactor Experiment, demonstrating VERA's effectiveness in multiphysics simulations of MSRs.

I. INTRODUCTION

In recent years, the nuclear community has seen a resurgence of interest in molten salt reactors (MSRs). MSRs can contribute to improved safety, as they operate at atmospheric pressure, and their use of molten fuel eliminates the possibility of fuel failures. Breeding and burning technologies could also allow for significant improvements to the typical once-through fuel cycle, as well as economic benefits and proliferation resistance. These advantages over light water reactor (LWR) systems make MSRs an intriguing technology, thus motivating renewed research and development efforts.

MSRs present several new modeling and simulation challenges not found in LWRs due to their molten, flowing fuel. The flowing fuel means that delayed heat precursors and delayed neutron precursors decay in locations other than where they were produced, often outside the core or after having flowed around the loop and back into the core through the inlet. Important parasitic absorbers such as ^{135}Xe and ^{149}Sm also flow, rendering traditional models for equilibrium concentrations inaccurate unless the movement of the fuel around the loop is properly accounted for. Additionally, the chemistry of the fuel becomes an important problem. The liquid fuel effectively produces the entire periodic table of elements from fission in a single molten solution, requiring new models to be developed and implemented to capture the generation and transport of chemical species.

The Virtual Environment for Reactor Applications (VERA) has been developed as part of the Consortium for Advanced Simulation of LWRs (CASL) (Ref. 1) to provide a high-fidelity multiphysics framework for LWR simulation and analysis. The development of the VERA tools has been focused on addressing a series of industry challenge problems that cannot be addressed using legacy methods. Recent successes using VERA to address multiphysics problems such as CRUD-induced power shift (CIPS)[2], combined with the fact that many of the methods are agnostic to the reactor being analyzed, have spurred efforts to extend the VERA tools for analysis of MSRs.

The remainder of this paper is organized into four sections. First, an overview of MSR physics and the

necessity for multiphysics simulations is presented. Next, the individual components of VERA are discussed, with an emphasis on the modifications for MSR modeling and simulations. Results are then presented to demonstrate the new capabilities. Finally, the paper concludes with some summary discussion of the current capabilities and ongoing work in the VERA tools.

II. MOLTEN SALT REACTOR MULTIPHYSICS

Traditional reactor analysis consists of two primary components: neutronics and thermal hydraulics (TH). The neutronics component consists of solving the neutron transport equation for the neutron flux due to both prompt and delayed neutrons. Included in this calculation is the isotopic transmutation that occurs in the fuel as a result of nuclear reactions and radioactive decay. The neutronics component of reactor physics can be summarized by Eqs. (1) through (3). For brevity, the equations are described only at a high level, rather than by providing detailed definitions of each term and variable. Most variables have their usual meaning.

$$\boldsymbol{\Omega}\cdot\boldsymbol{\nabla}\psi(\boldsymbol{r},\boldsymbol{\Omega},E)+\sum_{i}^{n_{iso}}N_i(\boldsymbol{r})\sigma_{t,i}(T,E)\,\psi(\boldsymbol{r},\boldsymbol{\Omega},E)=\int_0^{\infty}\int_{4\pi}\sum_{i}^{n_{iso}}N_i(\boldsymbol{r})\sigma_{s,i}(T,\boldsymbol{\Omega}'\cdot\boldsymbol{\Omega},E'\rightarrow E)\,\psi(\boldsymbol{r},\boldsymbol{\Omega}',E')d\Omega'\,dE' + \frac{1}{4\pi k_{eff}}\left(\int_0^{\infty}\sum_{i}^{n_{iso}}N_i(\boldsymbol{r})\left(1-\beta_{t,i}\right)\nu\sigma_{f,i}(T,\,E'\rightarrow E)\,\phi(\boldsymbol{r},E')dE'+\chi_D(E)\sum_{k=1}^{n_{prec}}\lambda_k C_k(\boldsymbol{r})\right). \tag{1}$$

$$\frac{dC_k(\boldsymbol{r})}{dt}=0=\int_0^{\infty}\sum_{i}^{n_{iso}}N_i(\boldsymbol{r})\beta_{k,i}\nu\sigma_{f,i}(T,\,E'\rightarrow E)\,\phi(\boldsymbol{r},E')dE'-\lambda_k C_k(\boldsymbol{r})-\boldsymbol{\nabla}\cdot C_k(\boldsymbol{r})\boldsymbol{v}(\boldsymbol{r}). \tag{2}$$

$$\frac{dN_i(\boldsymbol{r})}{dt}=\sum_{j=1}^{n_{iso}}\left(\gamma_{i,j}\lambda_j+\int_0^{\infty}\zeta_{i,j}\sigma_j(T,E')\phi(\boldsymbol{r},E')dE'\right)N_j(\boldsymbol{r})-\lambda_i N_i(\boldsymbol{r})-\int_0^{\infty}\sigma_j(T,E')\phi(\boldsymbol{r},E')dE'\,N_i(\boldsymbol{r}) -\boldsymbol{\nabla}\cdot N_i(\boldsymbol{r})\boldsymbol{v}(\boldsymbol{r})-\boldsymbol{\nabla}\cdot\boldsymbol{\mathcal{J}}_i(\boldsymbol{r},T)+\dot{F}_i(\boldsymbol{r}). \tag{3}$$

Equation (1) gives the steady-state neutron transport equation, separating out the prompt and delayed fission neutron in the last two terms. Equation (2) gives the delayed neutron precursor concentration C_k for each delayed group k as a function of space (and time in a time-dependent problem) due to production from fission and loss by radioactive decay. Equation (3) gives the change in nuclide concentration N_i for each isotope i over time due to loss by radioactive decay, production from fission, production from decay of other nuclides, and loss by parasitic absorption. The terms highlighted in red are specific to MSRs and are discussed in more detail later.

The TH component of reactor physics can also be summarized by three equations:

$$\boldsymbol{\nabla}\cdot\rho(T,P)\boldsymbol{v}(\boldsymbol{r})=0. \tag{4}$$

$$\boldsymbol{\nabla}\cdot\rho(T,P)\boldsymbol{v}(\boldsymbol{r})\boldsymbol{v}(\boldsymbol{r})=-\boldsymbol{\nabla}P(\boldsymbol{r})+\boldsymbol{\nabla}\cdot\mathcal{T}(\boldsymbol{r},T,P)+\rho(T,P)\boldsymbol{g}. \tag{5}$$

$$\boldsymbol{\nabla}\cdot\rho(T,P)\boldsymbol{v}(\boldsymbol{r})h(\boldsymbol{r})=-\boldsymbol{\nabla}\cdot q(\boldsymbol{r})+\mathcal{T}(\boldsymbol{r},T,P)\boldsymbol{\nabla}\colon\boldsymbol{v}(\boldsymbol{r})+\int_0^{\infty}\sum_{i}^{n_{iso}}N_i(\boldsymbol{r})\kappa\sigma_i(T,\,E')\,\phi(\boldsymbol{r},E')dE'. \tag{6}$$

Equation (4) gives the mass continuity equation; Eq. (5) gives the momentum conservation equation; Eq. (6) gives the energy conservation equation, with the last term being the heat production in the fluid due to nuclear reactions. For LWRs, these reactions are primarily the results of neutrons slowing down in the coolant, but MSRs have heating in the fluid due to fission as well.

Equations (1) through (6), neglecting the highlighted terms, show that the neutronics and TH are coupled primarily in the temperature and density feedback of the TH equation solutions into the neutron cross sections, which in turn affects the heat sources in the TH equations. Depending on the type of analysis being conducted, approximate solutions can sometimes be used to decouple the neutronics from the TH to simplify the solution methodology.

However, these simplifications cannot be made for MSRs because of the flowing fuel. The highlighted term in Eq. (2) describes the movement of the delayed neutron precursors in the flowing fuel after they are produced from fission. Traditionally, and throughout this paper, the delayed neutron precursors are divided into six groups with half-lives ranging from less than 1 second to around 1 minute. Because of this, the long-lived precursors, especially, are able to move significant distances from their points of production, impacting the reactivity and neutron flux distribution in the reactor.

Likewise, Eq. (3) has three highlighted terms that are unique to flowing fuel. The first, $-\boldsymbol{\nabla}\cdot N_i(\boldsymbol{r})\boldsymbol{v}(\boldsymbol{r})$, is analogous to the additional term added by Eq. (2), describing the movement of each nuclide from its point of origin due to the flowing fuel. The second term, $-\boldsymbol{\nabla}\cdot\boldsymbol{\mathcal{J}}_i(\boldsymbol{r},T)$ describes the interaction of each nuclide with system components, such as deposition, erosion, and corrosion on component surfaces. Finally, the $\dot{F}_i(\boldsymbol{r})$ term describes the change in nuclide concentrations due to direct

feed to (positive $\dot{F}_i(\boldsymbol{r})$) or removal from (negative $\dot{F}_i(\boldsymbol{r})$) the fuel salt for each nuclide.

These new terms introduce a far greater degree of multiphysics coupling between the neutronics and TH components of the reactor. Thus, accurate solutions to these equations can be achieved only by solving all of them simultaneously. Doing so necessitates modeling and simulation tools that are capable of tightly integrating each of the physics pieces into a single simulation.

III. VIRTUAL ENVIRONMENT FOR REACTOR APPLICATIONS

Because of VERA's demonstrated successes with multiphysics reactor simulations, it was decided to modify VERA to address MSR modeling and simulation needs. These modifications have focused on further development of the multiphysics coupling between two of the primary core simulation packages used by VERA: the TH code CTF (Ref. 3) and the deterministic neutron transport code MPACT (Ref. 4).

III.A. CTF

CTF uses the subchannel approach to solving the coupled mass, momentum, and energy equations for fluid flow through a reactor core. For LWRs, it solves these equations using a two-fluid (liquid and gas), three-field (liquid, vapor, entrained droplets) approach to account for boiling that occurs in the reactor. It also has an extensive coupling interface that allows external codes to control its setup and execution, as well as retrieve solution data such as fuel rod temperature distributions and coolant temperature and density.

Several improvements have been made to CTF to model MSRs. First, thermophysical properties tables for FLiBe and FLiNaK salts were added to the code. This was a necessary first step to get realistic solutions to the TH equations. Additionally, new geometry capabilities were added to allow CTF to model the whole primary loop instead of just the active core region. Momentum boundary conditions can be set to simulate the pump, and energy boundary conditions can be used to simulate the heat exchanger. These additions allow CTF to properly model the flow of the fuel salt out of the core, around the loop, and back in the inlet, which is a necessary feature of an MSR multiphysics simulation.

The most significant addition to CTF has been a new species transport module[5]. The mathematical details of this new module are deferred to the references, but a brief description is provided here. The species transport module allows CTF to track arbitrary species in the salt as the salt flows around the loop. In addition to the movement of the species, production and loss terms in the salt and transition terms between species are tracked. Boundary conditions can also be used to model an external source or sink for a given species. Coupling interfaces were implemented along with this work, allowing external codes to create an arbitrary number of species and set their source and transition terms so CTF can use the TH solution to perform the transport calculations.

Of particular note in the species transport model is the transported gas capability. This allows CTF to model gas injection into a molten salt system, calculating the number and sizes of bubbles in each mesh element of the CTF model. Other species that can exist in both liquid and gas phases are then allowed to interact with these inject gas bubbles, allowing them to grow and shrink based on the TH conditions and total amount of gas present. The transported gas bubbles are assumed to be moving the same speed as the fuel salt. This assumption could break down at high concentrations, but is likely reasonable for the applications of interest for this capability.

III.B. MPACT

MPACT uses the 2D/1D method to solve the neutron transport equation[6]. The 2D/1D method decomposes the problem into a stack of 2D planes, using the method of characteristics (MOC) radially to resolve complex geometry with high fidelity, then coupling each of the 2D planes axially using a fast, lower-order transport solver (usually P_3 wrapped in a nodal expansion method kernel). These calculations produce 3D pin-resolved neutron flux distributions throughout the core, typically in 51 energy groups. MPACT has already been coupled to CTF for LWR simulations as part of CASL's efforts[7], accomplishing detailed TH feedback in several hundred channels per fuel assembly. As part of the same work, MPACT was also coupled with SCALE's (Ref. 8) depletion module ORIGEN (Ref. 9), which provides pointwise fuel depletion calculations for each of millions of cross section regions in a full LWR model.

The first step in adapting MPACT for MSR analysis was to extend its geometry capabilities. One advantage of using MOC as the radial transport method in 2D/1D is that it is by nature geometry-agnostic, so the geometry extensions were necessary only in MPACT's infrastructure, not in the actual solver methods. These geometry extensions included support for cylindrical vat-like reactors and the Molten Salt Reactor Experiment (MSRE), among others.

One of the key features of MPACT in LWR simulation has been its highly detailed depletion calculations, calling the ORIGEN module for millions of cross section regions at each depletion timestep. For MSR simulation, the movement of the fuel introduces new effects in the depletion calculation. To handle this, a lumped depletion capability has been added to MPACT (Ref. 10). In this capability, it is assumed that the time scale for the fuel salt's movement through the core and around the primary loop (usually seconds or minutes) is

much shorter than the time scale for depletion calculations (usually weeks or months). Because of this, it can be assumed that the fuel is always well mixed and has a uniform isotopic distribution everywhere in the core. This gives the following equations:

$$\bar{\sigma}_{i,g} = \frac{\sum_j \sigma_{i,j,g}\phi_{j,g}V_j}{\sum_j \phi_{j,g}V_j} \quad , \qquad (7)$$

$$\bar{\phi}_{j,g} = \frac{\sum_j \phi_{j,g}V_j}{V_{salt}} , \qquad (8)$$

where subscripts *i*, *j*, and *g* indicate reaction type, mesh element in the active core region, and energy group respectively; σ is a cross section; ϕ is the scalar flux; and V is volume. Equation (7) is for the average reaction cross section in the salt, averaged over the entire active core region. Because the salt is assumed to be well mixed, a single cross section can be used for the entire salt. Likewise, a single flux can be used for the entire salt as well, as shown in Eq. (8). The flux is summed over the active core region but normalized by the total salt volume V_{salt} of the salt in the core and primary loop. This is done to account for the fact that the salt spends part of its time outside the active core region, away from any appreciable scalar flux. Thus, Eq. (8) calculates an effective flux rather than the actual flux. With these quantities, the entire salt can then be depleted in a single point depletion calculation using ORIGEN to capture the effects of the moving salt.

Along with the lumped depletion capability, a simple feed and removal capability was added. This feature allows the user to specify a particular isotope or element to add to a material or remove from a material. This can be done continuously or in batches during a depletion calculation. This capability also allows isotopes to be transferred between two different materials in cases where the MPACT model contains multiple salts or system components.

Improvements were also made to the TH coupling with CTF. The initial coupling implementation used a conformal coupling mesh in which both codes had knowledge of fuel rods centered in pin cells. All data was exchanged using this mesh as a reference point. However, MSRs do not typically have a regular lattice of rod-like structures as LWRs do, so the coupling approach for MSRs is much more general. Instead, new interfaces were added to CTF to expose the locations and dimensions of CTF's channel mesh. MPACT now maps its mesh regions to the appropriate CTF channel and calculates the heat source in each channel directly. CTF then returns TH solution data to MPACT on the channel mesh, with MPACT mapping the TH data to each mesh region as needed.

Finally, a new subpackage was added to MPACT to drive the species transport calculations and coupling with CTF. This package performs the calculations necessary to generate inputs to the species transport calculation, such as the direct yield of each species from fission, loss of each species due to radioactive decay or parasitic absorption, and direct addition and removal terms specified by the user.

The species transport coupling capabilities in MPACT currently support delayed neutron precursor drift, general isotope and element drift, and gas bubble injection and transport. If an element is specified, it is unfolded into its constituent isotopes and each of those isotopes is transported. For the fission yield, only direct yield from fission is accounted for. Production of an isotope via decay of another fission product is accounted for only if the parent isotope is also being tracked by the species transport. The user is responsible for specifying the appropriate parent isotopes to capture all significant effects of the species transport.

IV. RESULTS

This section presents the results of the lumped depletion and species transport coupling capabilities that have been added to VERA. First, a brief description of the MSRE is presented. Next, lumped depletion results are shown for the MSRE. Finally, a series of steady-state coupled species transport calculations using the MSRE model are shown for a variety of species.

IV.A. Molten Salt Reactor Experiment

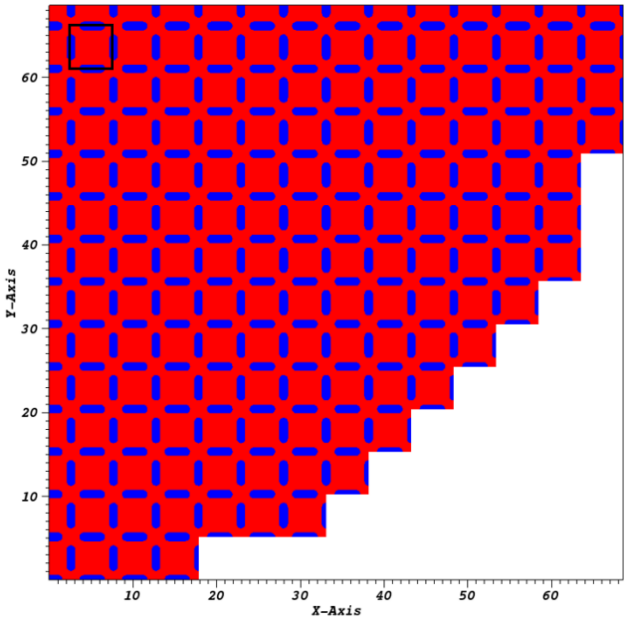

Fig. 1. A 2D slice of MPACT MSRE quarter core model showing fuel salt (blue) in graphite blocks (red) with MPACT unit cell outlined in black (dimensions in cm).

The MSRE (Ref. 11) was an experimental reactor operated at Oak Ridge National Laboratory (ORNL) from 1965 to 1969. It consisted of an array of graphite stringers in contact with one another, with salt channels machined into each of the four faces of the four stringers. The graphite served as the neutron moderator for the reactor. The fuel salt used in the reactor was 65% ^{7}LiF, 29.1% BeF_4, 5% ZrF_4, and 0.9% UF_4. The reactor typically operated at a thermal power level of approximately 7.4 MW and had a loop time of about 27 seconds. The geometry of the MSRE as modeled by MPACT is shown in Fig. 1. Because the MSRE is the only MSR to have operated and produced experimental data, it has served as the primary MSR model for the VERA MSR development and is used to show the results for the remainder of this paper.

IV.B. Lumped Depletion

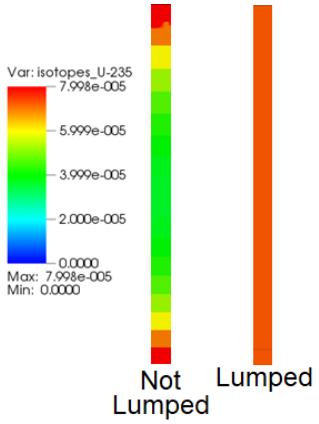

Fig. 2. Distribution of ^{235}U in a fuel channel for non-lumped (left) and lumped (right) depletion calculations.

In Fig. 2, the differences between lumped and non-lumped depletion are shown for a single channel. In the case of non-lumped depletion, the fuel in the center of the reactor is burned disproportionately quickly compared with the fuel in the lower-power regions at the top and bottom of the core. This is a physically non-sensical result. However, lumped depletion uses the well-mixed assumptions, resulting in a uniform isotopic distribution throughout the whole salt volume.

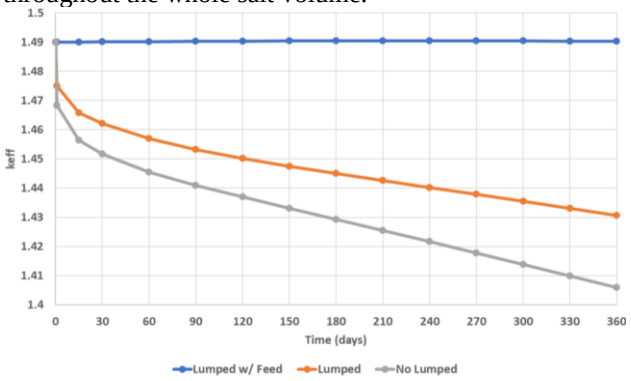

Fig. 4. Demonstration of lumped depletion and continuous fuel feed simulations in MSRE.

Fig. *4* shows the results of three different MSRE depletion calculations. The initial value of k_{eff} is around 1.49 due to the fact that the simplified model contains no structural or control materials and very little leakage. The gray line shows the depletion without lumped depletion. The orange shows the lumped depletion result. The difference in reactivity is large almost immediately, as the fuel burns more evenly in the lumped depletion case. After a year of depletion, there is more than a 2% different in reactivity from enabling lumped depletion. Finally, the blue line shows lumped depletion with a continuous feed of pure ^{235}U. A feed rate of 2.2×10^{19} atoms per day (~8.6 mg per day) was used to keep k_{eff} approximately constant. There is some deviation of around 100 pcm from the initial value, but this calculation demonstrates the potential to maintain criticality using a continuous fuel feed. Likewise, poisons could also be removed to maximize the reactivity with as little fuel as possible.

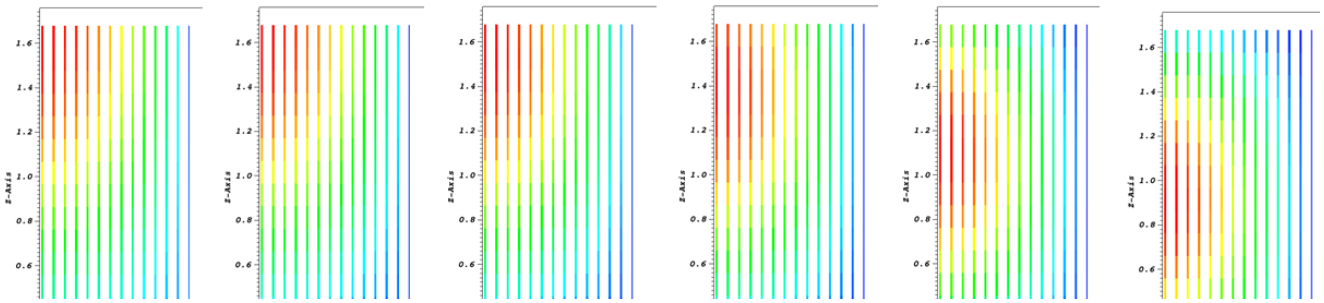

Fig. 3. Distribution of delayed neutron precursors in MSRE core for groups 1 (left) to 6 (right); half-lives are 55.45 s, 21.80 s, 6.36 s, 2.19 s, 0.51 s, and 0.08 s from left to right.

IV.C. Steady-State Species Transport

The species transport calculations are shown in three different sections. The delayed neutron precursor transport results are shown first, followed by isotope transport and gas bubble transport.

IV.C.1. Delayed Neutron Precursor Transport

Fig. 3 shows the distribution of delayed neutron precursors in the core for each of the six delayed groups. Groups 1–4 all show significant movement from the center of the core. The flow velocity in the MSRE was about 27 cm/s, and the active core region is about 160 cm tall. The shortest half-life in groups 1–4 is 2.19 s in group 4, so all four of these groups are able to travel a significant distance away from the center of the core where the power, and thus precursor production, is greatest. However, groups 5 and 6 have much shorter half-lives of 0.51 s and 0.08 s respectively, resulting in much less movement toward the top of the core. This is especially true of group 6, which almost exactly matches the power shape in the core.

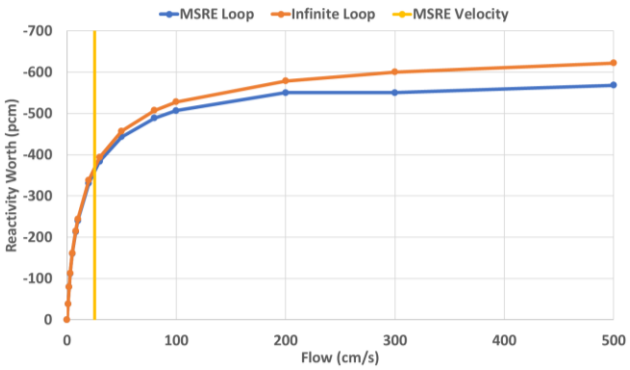

Fig. 5. Reactivity worth of delayed neutron precursors drift as a function of flow velocity.

Two different sets of calculations were performed using delayed neutron precursor transport coupling between MPACT and CTF. The first was the standard MSRE model, which has a primary loop length of about 560 cm outside the active core. The second was an "infinite" loop model in which precursors were not allowed to re-enter the core once they had exited. Each of these two models was simulated using flow velocities ranging from 0 to 500 cm/s. Fig. 5 shows the results of the two sets of calculations. At low flow velocities, there are no appreciable differences. However, as flow velocity increases, the infinite loop model begins showing a greater reduction in reactivity worth, reaching about a 50 pcm difference at very high flow velocities. This is due to the fact that in the normal model, some of the long-lived precursors are able to flow all the way around the primary loop and back in the inlet, whereas the infinite loop model assumes they all decay outside the core once they leave. The MSRE operated at a relatively low flow velocity, so the precursor re-entry effect was small, but non-zero.

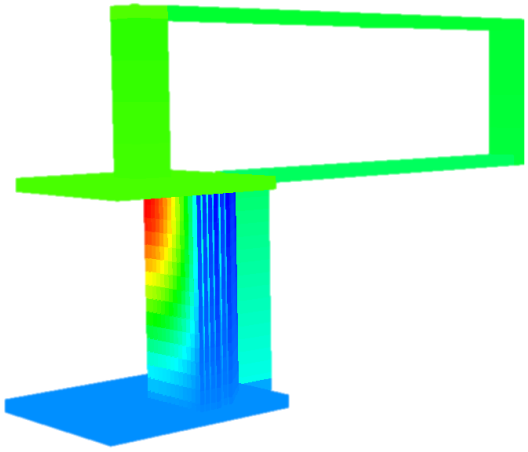

Fig. 6. Primary loop distribution of Group 1 delayed neutron precursors.

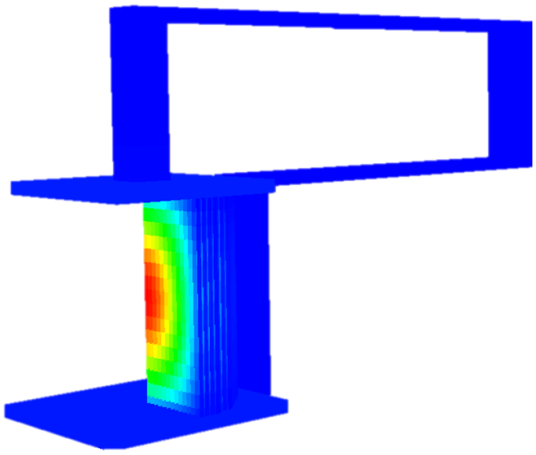

Fig. 7. Primary loop distribution of Group 6 delayed neutron precursors.

In Fig. 6 and Fig. 7, the distributions of the longest- and shortest-lived precursor groups, respectively, are shown for the whole primary loop. These plots clearly show the re-entry of the group 1 precursors into the core, whereas the group 6 precursors practically do not exist outside the active core region.

IV.C.2. Isotope Transport

The isotope transport is demonstrated by performing an equilibrium xenon calculation for the MSRE. For this calculation, ^{135}I and ^{135}Xe are tracked using CTF's species transport module. Xenon-135 is of interest because of its

very large thermal absorption cross section, and ^{135}I is of interest because it is a significant source of ^{135}Xe via radioactive decay. The species transport coupling for this demonstration includes the direct yield of both isotopes from fission, the loss of both isotopes through parasitic absorption, and the production of ^{135}Xe via the decay of ^{135}I.

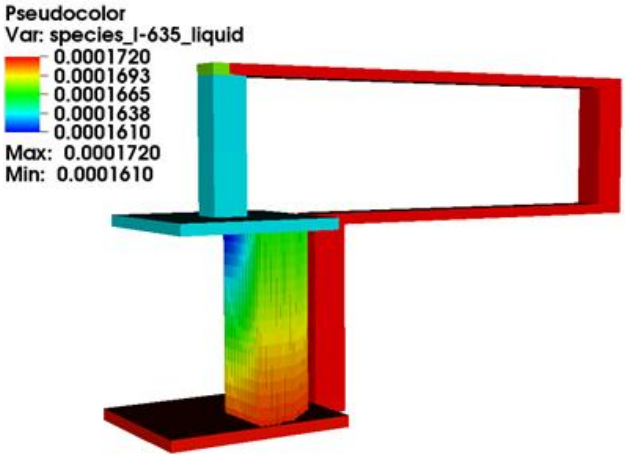

Fig. 8. Distribution of ^{135}I in primary loop of MSRE.

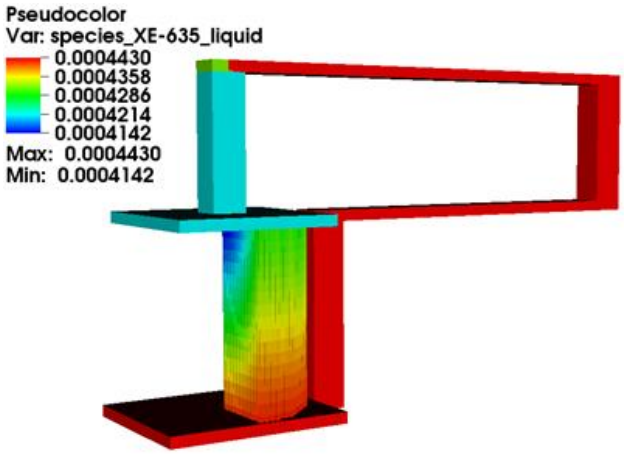

Fig. 9. Distribution of ^{135}Xe in primary loop of MSRE.

The results of the iodine and xenon transport calculations are shown in Fig. 8 and Fig. 9, respectively. The shape of the distribution is very similar between the two, with ^{135}Xe having a larger magnitude. The magnitude is due primarily to its 9.2-hour half-life compared with the ^{135}I half-life of 6.6 hours, causing the xenon to pile up more over time.

One feature of the iodine and xenon transport that is interesting compared with the delayed neutron precursors is that the peak of the distribution is outside the core, and the minimum of the distribution is at the top of the active core. The reason for this is the different time scales between the two types of species. The longest-lived delayed neutron precursors will travel around the loop only twice on average. However, iodine and xenon can travel around the loop many times before decaying. The most important component of the iodine and xenon concentrations is not the concentration that built in from fission during the most recent pass through the core, but rather the concentration built up from many passes through the core. Because of this, the fission production and loss terms in the core are relatively low compared with the total concentration of iodine and xenon in the coolant. The most significant effect on the concentration is the decrease in salt density as it heats up in the active core, which reduces the concentration of each constituent of the salt, including ^{135}I and ^{135}Xe. The heat exchanger in this model is at the very top of the loop above the active core, so the peak concentrations are reached when the salt is cooled and its density increased. These concentrations then remain nearly constant in the remainder of the external loop until the salt is heated again in the active core.

IV.C.3. Gas Bubble Transport

Fig. 10. Simplified MSRE loop void fraction due to helium gas bubble injection.

The final type of species currently supported in the coupling is gas bubble transport. In the MSRE, helium gas bubbles were injected into the primary loop and then removed later with an off-gas system. The purpose of this approach was to cause gaseous fission products with large

cross sections, such as xenon, to transport to the helium bubbles so they could be removed by the off-gas system. This improved the efficiency of fuel usage by reducing the loss of neutrons to parasitic absorption.

Modeling this capability in VERA with feedback into the neutronics is demonstrated through a simplified model of the MSRE. This model is a single graphite block with four half-channels, as shown by the black outline in Fig. 1. The core power levels, external loop geometry, and boundary conditions were scaled accordingly to produce core TH conditions similar to those in the full MSRE model.

Fig. *10* shows the void distribution in the simplified loop model due to helium gas bubble injection. The minimum in the void fraction occurs at the off-gas system. The bubbler is directly above the off-gas system, resulting in a peak in the void fraction at the top of the loop. The void concentration then decreases quickly as a result of the heat exchanger's effect on the salt density. It continues to drop gradually around the primary loop, then increases again in the active core region as the temperature rises.

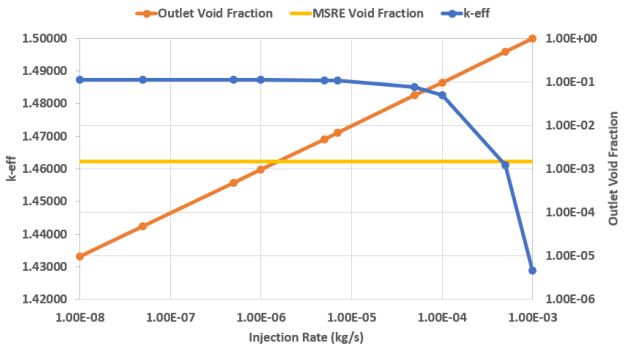

Fig. 11. Change in outlet void fraction and k_{eff} for MSRE simplified loop model.

Fig. *11* shows the change in both outlet void fraction and k_{eff} as a function of gas injection rate. The void fraction behaves exactly linearly as a function of injection rate. This is expected since the void is caused only by gas injection, not by coolant boiling as with some other reactors. The reactivity change is very small until the void surpasses 1%. At that point, k_{eff} begins to drop rapidly as a function of the gas injection rate. The yellow line shows the operating void fraction of the MSRE, about 0.15%. Thus, the reactivity effects of the helium injection are small for realistic injection rates. However, more significant effects can arise if other important neutron poisons interact with the helium bubbles and are removed via an off-gas system.

V. CONCLUSIONS AND ONGOING WORK

A brief overview of the need for tightly coupled multiphysics simulations for MSRs has been presented. The new features added to the VERA code suite to address these modeling needs were explained. Each of these features was then demonstrated using the MSRE, the only MSR to have been built and operated. The results of these calculations show the valuable information that can be obtained for MSR analysis using VERA because of the tight coupling that exists between the various physics packages.

Development work will continue on each of these capabilities, further improving the quality and usability of VERA for MSR analysis. Work will be done on the lumped depletion and species transport capabilities to ensure that they can operate together consistently. Care must be taken to ensure that the depletion and species transport are not "double counting" certain isotopes, especially through external addition and removal. A greater variety of species will also be supported by the coupling in the near future. Decay heat precursors, which create a heat source in the primary loop outside the active core that affects the TH solution, will be added. Additionally, support for multi-phase species and their interactions with the transported gas bubbles will be added. This work will enable a complete picture of the composition and TH conditions of the fuel salt everywhere in the active core and primary loop while accounting for a wide variety of operational conditions and procedures.

ACKNOWLEDGMENTS

Research sponsored by the Laboratory Directed Research and Development Program of Oak Ridge National Laboratory, managed by UT-Battelle, LLC, for the US Department of Energy.

REFERENCES

1. "Consortium for Advanced Simulation of Light Water Reactors (CASL)," Available online: URL https://www.casl.gov/.
2. B. COLLINS and J. GALLOWAY, "Mongoose Methods and Theory," ORNL Tech. Rep. CASL-U-2017-1354-000 (2017).
3. R. SALKO et al., *CTF Theory Manual*, The North Carolina State University (2017).
4. B. COLLINS et al., "Stability and Accuracy of Three-Dimensional Neutron Transport Simulations Using the 2D/1D Method in MPACT," *Journal of Computational Physics*, **326**, pp. 612-628 (2016).
5. Z. TAYLOR, "Implementation of Multi-phase Species Transport into VERA-CS for Molten Salt Reactor Analysis," Master's thesis, University of Tennessee, Knoxville, TN, USA (2019).

6. MPACT DEVELOPMENT TEAM, “MPACT Theory Manual, 2.2.0,” Oak Ridge National Laboratory Tech. Rep. CASL-U-2016-1107-000 (2016).
7. B. KOCHUNAS et al., “VERA Core Simulator Methodology for Pressurized Water Reactor Cycle Depletion,” *Nuclear Science and Engineering*, **185**, 1, pp. 217-231 (2017).
8. “SCALE: A Comprehensive Modeling and Simulation Suite for Nuclear Safety Analysis and Design,” ORNL Tech. Rep. ORNL/TM-2005/39, Version 6.1, available from Radiation Safety Information Computational Center at Oak Ridge National Laboratory as CCC-785 (2011).
9. I. GAULD et al., “Isotopic Depletion and Decay Methods and Analysis Capabilities in SCALE,” *Nuclear Technology*, **174**, 169 (2011).
10. C. GENTRY, B. BETZLER, and B. COLLINS, “Initial Benchmarking of ChemTriton and MPACT MSR Modeling Capabilities," *Transactions of the American Nuclear Society*, **117**, Washington, D.C., USA (2017).
11. M. ROSENTHAL, “An Account of Oak Ridge National Laboratory’s Thirteen Nuclear Reactors,” ORNL Tech. Rep. ORNL/TM-2009/181 (2010).